NATURAL NITRATE REMOVAL IN SHALLOW SUBSURFACE STREAM FLOWS

ABIGAIL HEATH

46 Pages

As agricultural growth increases across the planet, more anthropogenic nitrate from fertilizers and sewage effluent is contributed to the aquatic system, exacerbating both ecosystem- and human-health issues. Nitrate is naturally processed and removed within the environment, and those processes have been observed in a segment of substrata and porewater below streams called the hyporheic zone (HZ). The interaction of stream water with groundwater can promote denitrification; however, the rate of nitrate removal within the HZ is unknown. This study determined the extent of surface water-groundwater interactions in a HZ and assessed the nitrate removal in this zone via monthly sampling of three wells inserted along the length of T3, a stream located in the agriculturally dominated, Central Illinois landscape. Samples were taken from 10, 20, 30, and 50 cm below the streambed, the stream, and a groundwater well from spring to fall of one year to assess the full mixing patterns and nitrate contributions of the landscape to the stream system. The chemical composition of the stream water, groundwater, and HZ waters were analyzed using an Ion Chromatograph and applied in a mixing-model.

Results show that stream water and groundwater contribute proportionally inverting amounts to water flow through the depth of the HZ. The conservative ion chloride is a chemical indicator of mixing in waters, and in the studied HZ, chloride concentrations were 48.8% higher in surface water than groundwater, and a gradient of change between these two endmembers was observed along depth throughout the HZ. Decreasing nitrate as nitrogen (NO_3-N) levels along depth can be positively correlated to this gradient of mixing in the HZ. This relationship supports

that the mixing of surface water and groundwater that occurs along the depth of the HZ thoroughly circulates surface water and removes its excess nitrate. A better understanding of how different water sources contribute to the HZ and how that water flows through this zone will better equip regulators and remediators to use streams and their hyporheic zones to remove excess nitrate from agricultural runoff, contributing to healthier ecosystems and drinking water.
KEYWORDS: hyporheic zone, mixing, nitrate, stream restoration

NATURAL NITRATE REMOVAL IN SHALLOW SUBSURFACE STREAM FLOWS

ABIGAIL HEATH

A Thesis/Dissertation Submitted in Partial

Fulfillment of the Requirements

for the Degree of

HYDROGEOLOGY, M.S.

Geography, Geology, and the Environment

ILLINOIS STATE UNIVERSITY

2021

NATURAL NITRATE REMOVAL IN SHALLOW SUBSURFACE STREAM FLOWS

ABIGAIL HEATH

COMMITTEE MEMBERS:

Dr. Eric Peterson, Chair

Dr. Catherine O'Reilly

Dr. Wondwosen Seyoum

ACKNOWLEDGMENTS

Thank you to my committee, Dr.'s Eric Peterson, Catherine O'Reilly, and Wondy Seyoum. Thank you to the city of Bloomington, IL for access to the T3 site and The Illinois Groundwater Association and Illinois Lakes Management Association for the generous funding provided for this project. Thank you also to my field assistants Caitlin Noseworthy, Cavien Satia, Jack Wassik, and Eli Schukow.

<A.A.H.>

CONTENTS

TABLES

FIGURES

CHAPTER I: INTRODUCTION

As agricultural growth increases across the planet, more anthropogenic nitrate from agricultural fertilizers and sewage effluent is contributed to the aquatic system. Nitrate naturally occurs in the environment, but because it is so necessary to ecological production, greater quantities are applied to the environment every year, via sources like nitrogen-rich fertilizers, to further increase biological production. The amount of net nitrogen-rich fertilizers alone entering the environment increased from approximately zero in 1945 to 850,000 Mg N/year in 2000 and as of 2016, had increased again to 16,252 kg/km^2 on corn crops alone in the U.S., magnitude greater than in previous years (Turner and Rabalais, 1991; David and Gentry, 2000; Piske and Peterson, *In Review*). This is especially relevant in the Midwest, where more than half of land use is cropland and nitrogen inputs via fertilizer are some of the highest in the United States (David and Drinkwater, 2010; USDA, 2019). In moderation, nitrate can contribute to a thriving ecosystem, but in excess of the 10 mg/L nitrogen-as-nitrate maximum contaminant level established by the USEPA, nitrate in the environment can be detrimental to both ecosystems and humans (USEPA, 2020). Excess nitrogen from nitrate can cause algal blooms, which lead to anoxic zones in aquatic environments. Toxic levels of nitrate can also cause health complications for humans when ingested, such as blue baby syndrome (CDC, 2015).

Nitrate is naturally processed and removed within the environment. Nitrification is the process by which ammonia oxidizes to become nitrate. Denitrification occurs when nitrate reduces to dinitrogen (N_2). These two processes contribute to the cycle that balances the level of nitrate in the environment, especially denitrification, which requires a saturated, low-oxygen environment with dissolved organic matter to occur; this is converse to the warm, oxygenated environment required by nitrification (Maas et al., 2019). Both nitrification and denitrification

take place fairly exclusively in soils. While microbes are the vital component for the initiation of both of these processes, plant roots play a key role in tandem with localized symbiotic bacteria in the soil to aid in the denitrification process (Vitousek et al., 2002; Baker and Vervier, 2004; Puckett et al., 2008; Ward, 2013). The denitrification process has also been observed in a segment of substrata and porewater below streams, where stream water and shallow subsurface waters interact, called the hyporheic zone (HZ).

Plants, which depend on the key nutrient of nitrogen-as-nitrate, uptake nitrate in soil while avoiding nitrite, which lowers nitrate concentrations further in abundantly vegetated zones (Sabater et al., 2003; Zak et al., 2018). Aquatic systems such as wetlands, which specifically have a constantly high level of available biomass and consistent burial and deoxygenation of substrata, have been a confirmed sink for excess nitrate in the environment (Van der Hoven et al., 2008;Seeger et al., 2013, Ackerman et al., 2015). Vegetation in and around streams, especially on the banks and within the riparian zone of streams, have a high capacity for nitrate assimilation, the process by which plants uptake. In some studies, plants have been observed to remove up to 50% of the nitrate being carried into streams via runoff (Clausen et al., 2000; Sabater et al., 2003).

The geomorphology of a stream and the physical conditions of its HZ determine how much nitrate removal occurs in a stream's HZ. An optimal HZ ensures a longer residence time for water in the zone to be able to fully interact with the zone sediments, microbes, and plants and is manifested best in meandering streams (Zaramella et al., 2003; Lautz and Fanelli, 2008; Zarnetske et al., 2011; Peterson and Benning, 2013). Stream bed sediments and structures that support HZ denitrification are those which confine the waters to a more focused area and extend the residence time of that water in the HZ (Peter et al., 2019). There are many kinds of sediment

makeups and stream morphological structures that support this, including a clay layer in the stream bed, a low-gradient or riffle-heavy stream topography, and the previously mentioned stream meanders (Hill et al., 1998; Puckett et al., 2008; Krause et al., 2013). Sediment types that are especially effective for denitrification not only confine HZ water and extend its residence time in the stream bed, but contribute organic matter to the system, such as sandy-silty stream bed matrices (Pescimoro et al., 2019). However, because of its general lower concentration of oxygen, the contribution of groundwater to the system can be just as significant as denitrification due to plant root uptake in shallow subsurface and riparian environments. A system which allows for greater mixing with groundwater and which experiences deeper infiltration of nitrate-rich surface waters to groundwater-dominant levels of the HZ will exhibit more significant denitrification (Smith and Tiedje, 1979; Mason et al., 2012; Krause et al., 2013; Ackerman et al., 2015).

Because of the requirements for denitrification, the extent to which this process occurs in a stream varies greatly based on the oxygen level in the water and the HZ (Maazouzi et al., 2013; Boulton et al., 1998). One expects to see more oxygen in surface waters and less oxygen in ground waters. This is key both to the ability to recognize the contribution of groundwater versus surface water to the HZ and to the extent of that contribution to nitrate processing in this zone. If there is more groundwater upwelling than surface water downwelling then there will be less oxygen in the HZ and therefore more denitrification occurring. The converse is also expected to be seen. Also, it is expected that along the depth of the HZ, more surface water, and therefore more dissolved oxygen, will be seen in the porewaters near the stream bed surface while much less surface water input and more groundwater input will be seen at depth, where an associated lack of dissolved oxygen will be found (Hill et al., 1998; Zarnetske et al., 2011). A decrease in

dissolved oxygen concentration along depth is expected to correlate to an increase in nitrate removal along depth.

To try to estimate the amount of nitrate reduction seen along depth in the HZ, the amount of physical mixing between surface water and groundwater in this zone must be quantified. Conservative chemical tracers can be used as a proxy to model that physical movement of water, because they do not change in concentration due to varying environmental processes. Chloride, specifically, is present in the T3 environment, and has been previously used to model mixing of different water sources to the HZ (Triska et al., 1989; Peterson and Hayden, 2018).

Another indicator that mixing is occurring in the HZ and that the HZ environment is optimal for nitrate removal is temperature. Temperature at surface is expected to oscillate from cool in late fall to early spring and warm in spring to early fall, but a more consistent temperature should be observable in groundwater (Lapham, 1989; Ren et al., 2019). Shallow groundwater (groundwater shallower than 10 m in depth) can be separated into two zones. The first is the surficial zone, consisting of water located anywhere up to about 1.5 m in depth, which is affected by the same seasonal changes in temperature and precipitation events that affect the surface water temperatures. Deeper than 1.5 m, groundwater remains much more stable in temperature (Anderson, 2005). At the T3 study site specifically, the groundwater temperature ranges from 0°C to 19.6°C at the depth of 7.5ft (228.6 cm) and 0°C to 20.4°C at 5ft (152.4 cm), with fluctuations between the two extremes seen throughout the seasons. The HZ falls under this categorization of shallow groundwater, and the difference between the temperature of surficial zone shallow groundwater versus more general groundwater to the HZ can be used as a tracer for mixing of these two sources.

Depending on climate and season, stream stage will also vary throughout the year, usually having a higher water level in the winter and spring and a lower water level in the summer and fall. The water level of the stream and general hydration of the stream bed and surrounding soils will affect how quickly and effectively water infiltrates into the HZ and deeper water table as well as the amount that groundwater upwells and mixes with stream water. It can also contribute to a complex shift in the chemistry of both stream water and HZ water. A higher stream stage is associated with greater precipitation and a greater carrying capacity of dissolved organic carbon. This increased organic matter being deposited on the stream bed, in addition to a thicker stream water-groundwater interface, means that there is a thicker zone of organic-rich, anoxic material for denitrification to take place in, and more denitrification is expected to be seen during a period of high stream stage (Baker and Vervier, 2004). Periods with the warmest temperatures and highest stream stage will see optimal denitrification conditions in the substrata.

The transport and fate of nitrate is highly controlled by streams and this study will focus on analyzing particular physical processes in a stream to determine their contribution to nitrate removal in stream environments. The stream that will be studied for this project, T3, is a modified, low-gradient, third-order stream located in an agriculturally-rich region of central Illinois, making it a quintessential example of the streams found in high nitrate-producing agricultural lands seen throughout the Midwest (Hill et al., 1998; Peterson and Benning, 2013). The goal of this study is to answer the following questions:

1. What percent of water contributing to hyporheic flow in a stream originates from surface water flow and groundwater flow?
2. What is the trend of nitrate removal vertically and longitudinally in the subsurface below streams?

3. How far does stream hyporheic flow extend into riparian subsurface storage and how does this contribute to the removal of nitrate or lack thereof seen in question #2?

This study will determine the extent of surface water-groundwater interactions in stream beds and how those interactions contribute to nitrate movement through the environment by analyzing the chemical composition of the stream water and groundwater flowing through the hyporheic zone from spring to fall. It is hypothesized that stream water and groundwater contribute proportionally inverting amounts to water flow through the depth of the hyporheic zone and the chemistry of this mixing water contributes to nitrate removal from water in the HZ. A better understanding of how different water sources contribute to the HZ and how that water flows through this zone will better equip regulators and remediators to use streams and their hyporheic zones to remove excess nitrate from agricultural runoff, contributing to healthier ecosystems and drinking water.

CHAPTER II: METHODS

Study Site Description

This study observed and analyzed the mixing of waters within the hyporheic zone of tributary 3 (T3), a low-gradient, third-order stream located in an agricultural region of central Illinois. (Figure 1).

The T3 floodplain has a fairly shallow substrata, made-up with organic-rich sandy loam overlying a thin, heterogenous sandy gravel layer. The sand-gravel layer overlies an impermeable layer of glacial till (diamicton) at approximately two-meters depth (Figure 2) (Miller et al., 2019). T3 is incised about 1.5 m into the floodplain and exhibits a much shallower stratigraphic profile, with an approximately 40 cm-thick sandy, heterogenous layer overlaying the impermeable glacial till, which begins at about 40-50 cm in depth.

The physical characteristics of T3, specifically its size, morphology, gradient, and land use type represent a common stream type seen throughout the Midwest. It has been previously modified; a common practice seen with streams in heavily agricultural areas throughout the Midwest. It is surrounded by cropland, where excess nitrate input to streams via runoff is high due to crop fertilization. It is expected that the full processing capacity of a stream this size in such an environment can be observed in this stream (Peterson et al., 2001; Peterson and Benning, 2013).

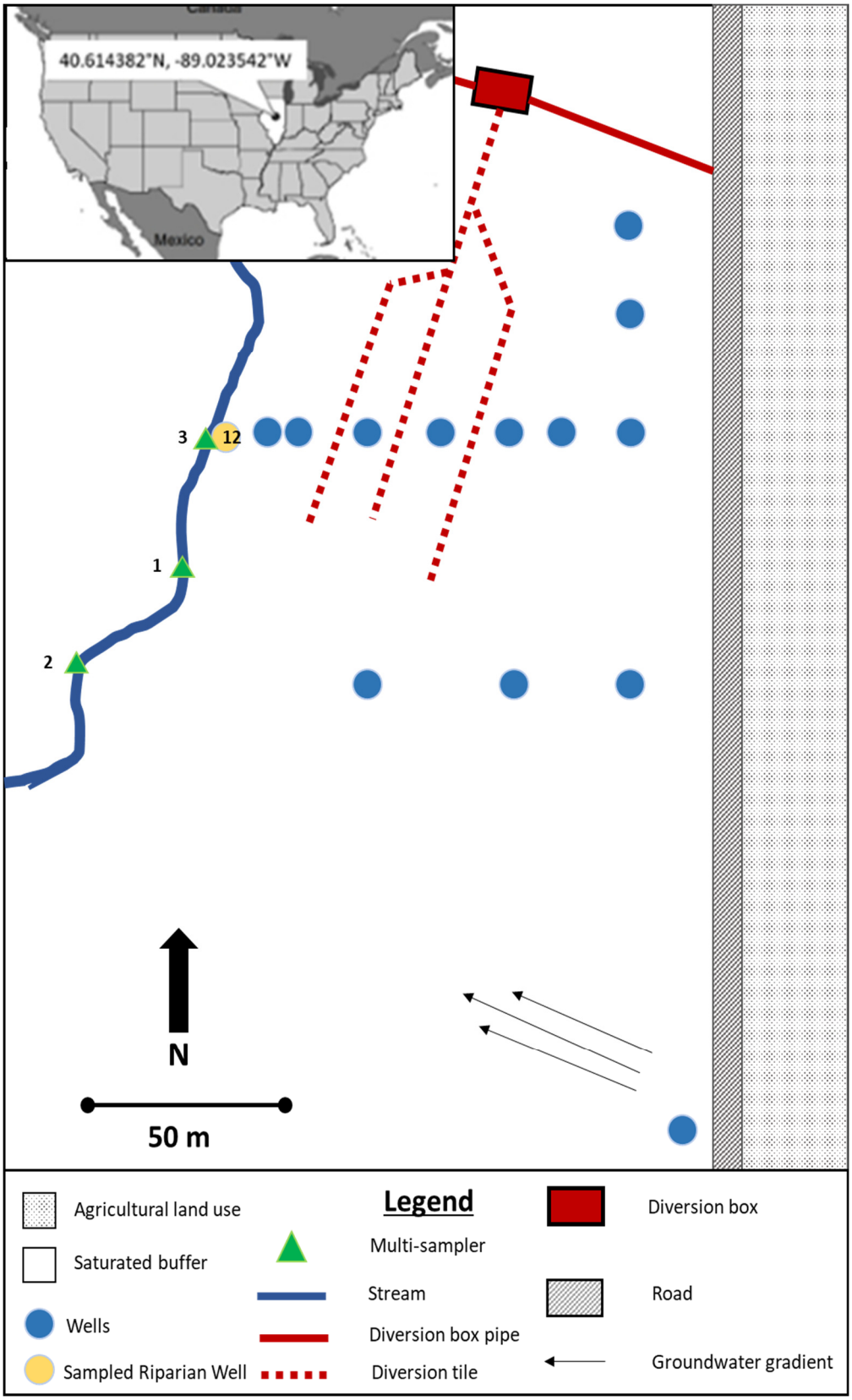

Figure 1 Map of the T3 study site and its well locations.

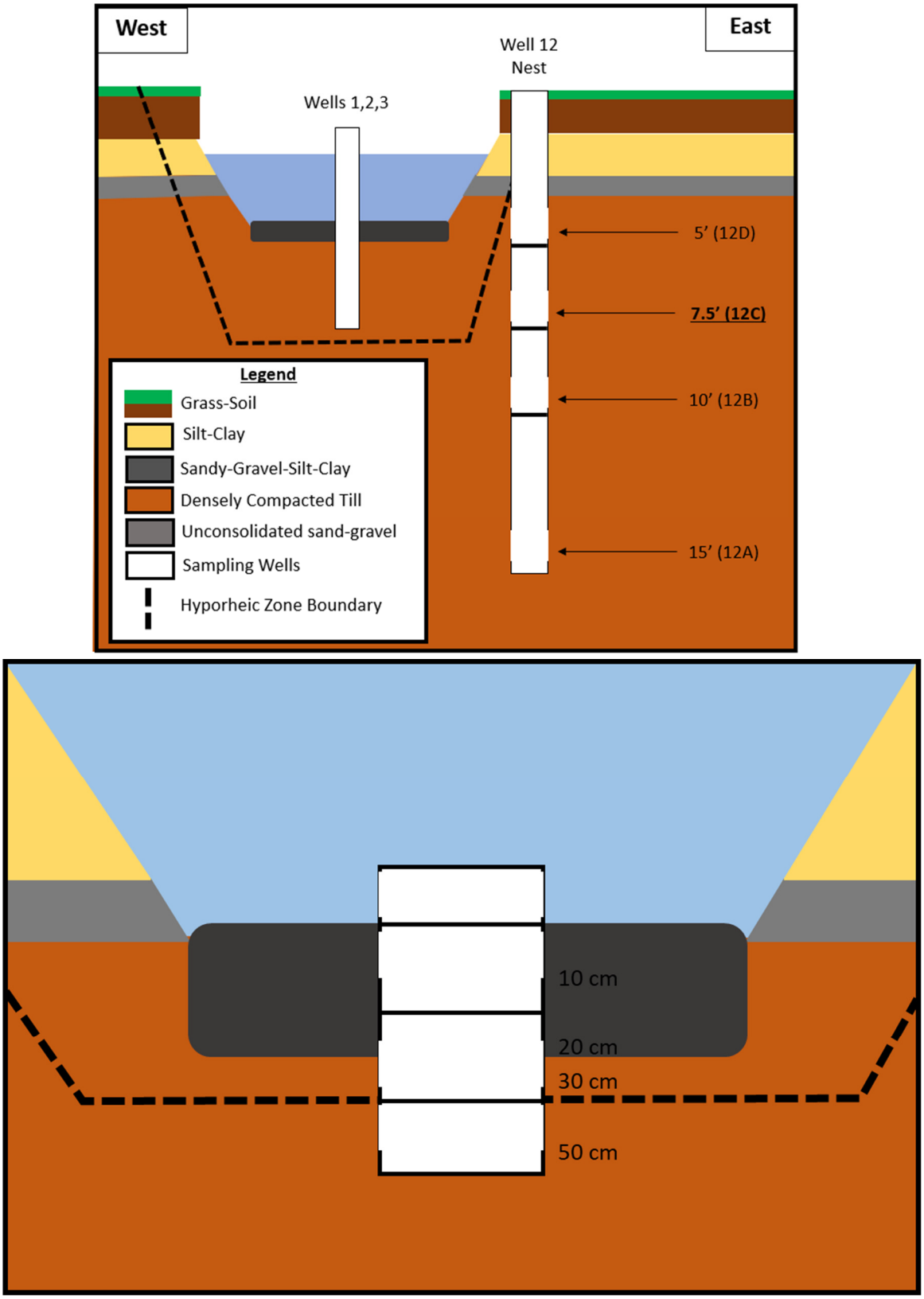

Figure 2 (top) Diagram of stratigraphy and in-stream and riparian well orientations at the T3 site. (bottom) Diagram of in-stream multi-sampler well layout.

Stream Sampling

Multi-level samplers were installed in the streambed in Spring 2020 at five-meter intervals. The samplers allow water to be drawn at 10 cm, 20 cm, 30 cm, and 50 cm depth (Figure 2). Using a peristaltic pump, water was drawn into 60 ml acid-washed sample bottles. A stream water grab sample was also taken during each sampling event. Grab samples from well 12C (7.5-ft or 228.6-cm depth) were also collected during each sampling event to represent the riparian groundwater endmember within the system. Due to COVID-19 travel restrictions and a particularly dry autumn (NIDIS, 2020), water samples were not collected in the spring months preceding June 2020 or in October 2020. Therefore, sample collections were conducted in June, July, August, September, and November of 2020, as well as in March 2021 rather than March 2020.

The samples were kept in a cooler in-field and immediately transported back to Illinois State University and frozen on the date of collection. In-situ measurements of dissolved oxygen concentrations were taken in the stream and the riparian, groundwater wells using a field YSI probe.

The collected samples were then thawed, filtered through a one (1) μm membrane filter and analyzed for NO_3-N and major anions (chloride, bromide, and sulfate) concentrations using an Ion Chromatograph. Quality Assurance (QA) and quality control (QC) were maintained during the analysis of water samples by running continuing calibration verification (CCV), blanks, and duplicates; the analytical error was less than 3%.

Model Development

To further support the determination of the contribution of groundwater versus surface water, a two-component mixing model of the waters within this environment was conducted. The two

endmembers of this model are groundwater (12C) and surface water (stream). Two model equations (Equation 1 and 2), were employed to calculate the percent of infiltrating surface water and the expected amount of NO_3-N at each depth in the HZ.

$$(Equation\ 1): \%SW = \frac{(Cl_{HZ} - Cl_g)}{(Cl_s - Cl_g)} \times 100$$

$$(Equation\ 2): NO_3N = \%SW\left(N_s - N_g\right) + N_g$$

The percent of surface water (%SW) for each depth was calculated using the measured chloride concentrations from field samples. As a conservative ion, chloride serves as a proxy for water movement and mixing in the environment. The %SW water was then used to calculate the expected NO_3-N to be seen at each depth within the HZ. In Equation 1, Cl_{HZ} represents the average measured chloride concentration in the HZ at T3 (mg/L). Cl_g represents the average measured chloride in the groundwater at T3 (as collected from the 12C well) (mg/L). Cl_s represents the average measured chloride concentration in the surface water (stream) at T3 (mg/L). %SW represents the calculated concentration of infiltrating surface water in the system. In Equation 2, while %SW represents that same value as in Equation 1, N_s represents the average measured concentration of NO_3-N seen in the surface water at T3 (mg/L) and N_g represents the average measured concentration of NO_3-N seen in the groundwater at T3 (mg/L) (Peterson and Hayden, 2018). The expected and measured NO_3-N concentrations were compared to assess the fate of nitrate. Processing of NO_3-N in the system is highlighted where the expected results do not match the measured results. Where the measured chloride concentrations in the HZ did not fall within the range of the measured endmember chloride concentrations, the expected NO_3-N could not be modeled.

CHAPTER III: RESULTS

Sampling Limitations

The COVID-19 pandemic impacted the accessibility to field sites and lab equipment during this study. Research travel was not allowed until summer 2020. This not only impacted when the sampling season began in the study's main field season of spring to fall of 2020, so that spring samples were collected the year following the summer and fall samples collected during 2020, but it also meant that the entire sampling season was pushed later into the year than previously planned. Because of this, most spring samples from March, April, and May were not able to be collected (March 2021 substituted for March 2020 in this study). Additionally, the summer and fall of 2020 were a drought-dominated time period in Illinois (NIDIS, 2020). Drought conditions exacerbated the lack of sampling during August and October, while the T3 stream exhibited a low, stagnant stage that would not have provided meaningful observations of water exchange and nitrate processing beyond that which was collected during the months that were sampled.

Observed Conditions of Chloride and Nitrate as Nitrogen

Surface Water

A mean of 25.31 mg/L of chloride was seen at surface in the T3 stream during the study (Table 1; Figure 3). In June 2020, the concentrations of chloride in the stream ranged from 31.12 mg/L to 34.26 mg/L. The July 2020 concentrations of chloride in the stream ranged from 23.29 mg/L to 31.61 mg/L. In September 2020, the concentration of chloride in the stream was 6.20 mg/L. In November 2020, the concentration of chloride in the stream was 20.70 mg/L. In March 2021, the concentration of chloride in the stream was 29.86 mg/L.

Table 1: Averages For Endmember Chemical Composition

Endmember	Month	NO_3-N	Cl^-	$SO4^{-2}$
Surface Water	June	15.84	32.69	20.15
Surface Water	July	8.67	26.40	19.63
Surface Water	September	BDL	6.19	13.84
Surface Water	November	1.25	20.69	49.55
Surface Water	March	7.36	29.86	22.95
Surface Water	Total Mean	9.37	25.31	22.80
Groundwater	June	0.73	4.60	347.42
Groundwater	July	0.96	4.03	143.49
Groundwater	September	0.41	4.39	32.81
Groundwater	November	0.33	4.24	66.55
Groundwater	March	4.27	5.86	18.55
Groundwater	Total Mean	1.00	4.34	150.93
Hyporheic Waters	June	8.79	23.31	23.17
Hyporheic Waters	July	4.95	18.18	16.50
Hyporheic Waters	September	0.29	9.66	16.23
Hyporheic Waters	November	0.48	9.25	15.37
Hyporheic Waters	March	1.89	13.15	30.54
Hyporheic Waters	Total Mean	4.08	14.77	20.23

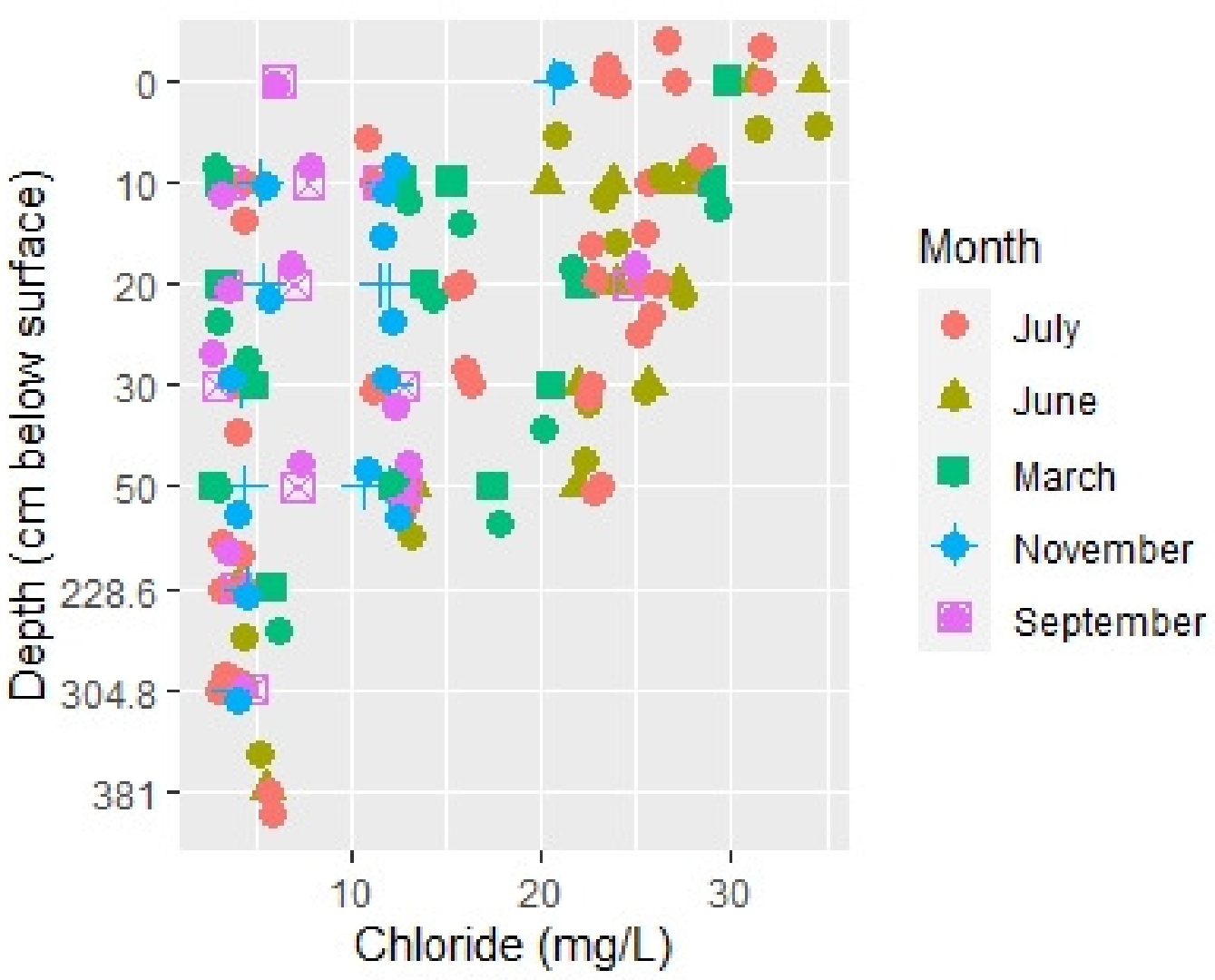

Figure 3 Measured Chloride concentrations along depth in the Hyporheic zone as compared to the riparian wells 5, 7.5. and 12 ft (228.6, 304.8, and 381 cm depth, respectively) at T3 during the sampling season in 2020.

A mean of 9.37 mg/L of NO_3-N was observed in the T3 stream (Figure 4). In June 2020, the concentrations of NO_3-N in the stream ranged from 15.06 mg/L to 16.64 mg/L. In July 2020, the concentrations of NO_3-N in the stream ranged from 7.86 mg/L to 10.70 mg/L. In September 2020, the concentrations of NO_3-N in the stream were below detection limit. In November 2020, the concentration of NO_3-N in the stream was 1.26 mg/L. In March 2021, the concentration of NO_3-N in the stream was 7.36 mg/L.

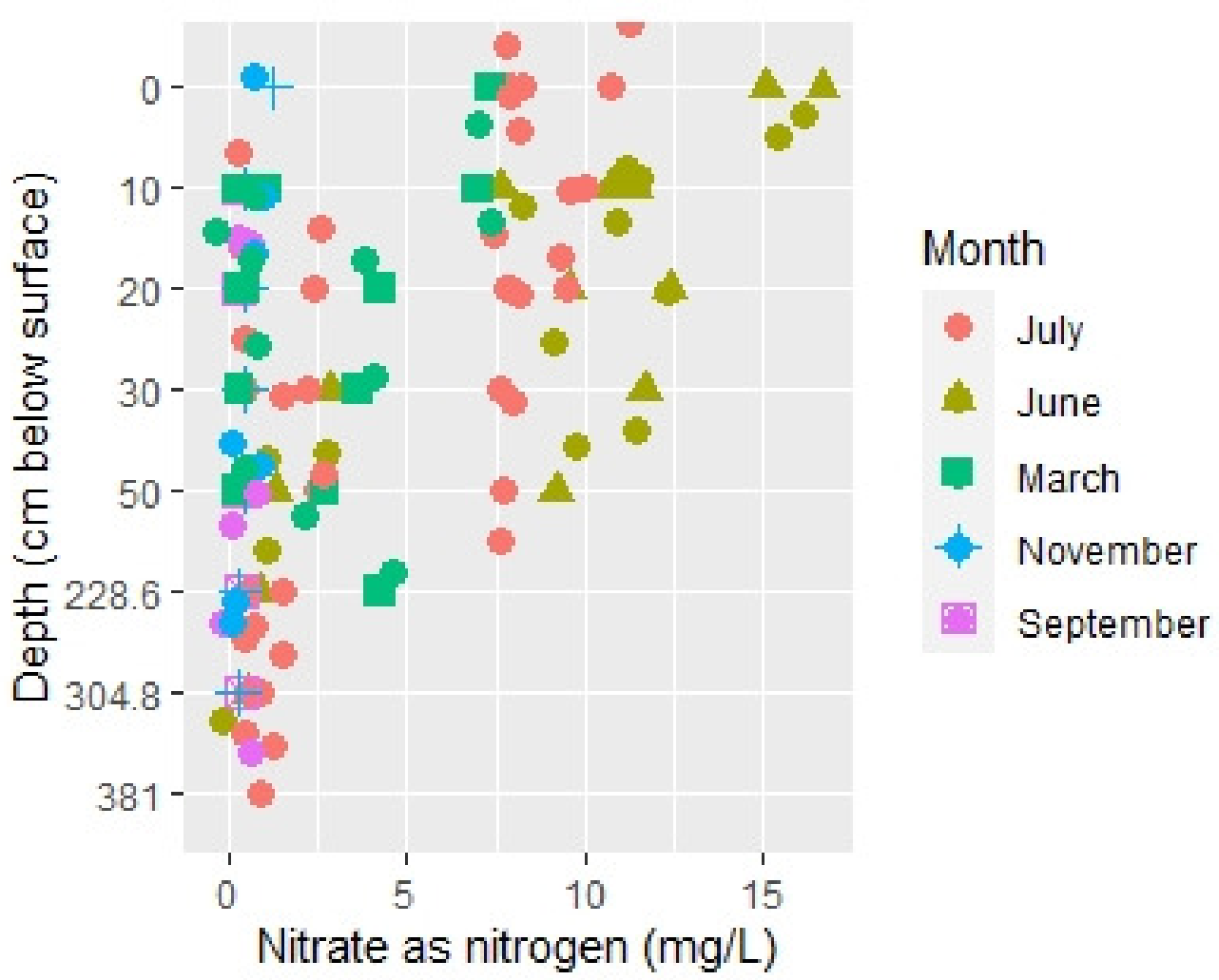

Figure 4 Nitrate as nitrogen along depth in the Hyporheic zone as compared to the riparian wells at T3 throughout the sampling season of 2020.

Groundwater

The 7.5 foot (228.6 cm)-deep riparian zone well samples, representing the groundwater endmember in this study, showed the lowest levels of both chloride and NO_3-N at the site; chloride was a mean of 4.35 mg/L in this zone and NO_3-N was a mean of 1.00 mg/L (Figure 3,4). In June 2020, the concentration of chloride in the groundwater was 4.05 mg/L. In July 2020, the concentrations of chloride in the groundwater ranged from 3.22 mg/L to 4.39 mg/L. In

September 2020, the concentration of chloride in the groundwater was 3.98 mg/L. In November 2020, the concentration of chloride in the groundwater was 4.60 mg/L. In March 2021, the concentration of chloride in the groundwater was 5.86 mg/L.

In June 2020, the concentration of NO_3-N in the groundwater was 0.89 mg/L. In July 2020, the concentrations of NO_3-N in the groundwater ranged from 0.60 mg/L to 1.51 mg/L. In September 2020, the concentration of NO_3-N in the groundwater was 0.41 mg/L. In November 2020, the concentration of NO_3-N in the groundwater was 0.34 mg/L. In March 2021, the concentration of NO_3-N in the groundwater was 4.27 mg/L.

The Hyporheic Zone

In the HZ of the stream, a mean of 14.77 mg/L of chloride and 4.08 mg/L of NO_3-N were observed. Along depth within the HZ, 20 cm depth showed the highest levels of both chloride and NO_3-N, while 30 and 50 cm depth showed the lowest levels and 10 cm depth showed the second highest levels of both ions (Appendix A).

A mean of 15.63 mg/L of chloride was observed at 10 cm below the streambed (Figure 3). In June 2020, the concentrations of chloride at 10 cm below surface ranged from 20.33 mg/L to 28.20 mg/L. In July 2020, the concentrations of chloride at 10 cm ranged from 4.48 mg/L to 28.62 mg/L. In September 2020, the concentrations of chloride at 10 cm ranged from 3.57 mg/L to 11.47 mg/L. In November 2020, the concentrations of chloride at 10 cm ranged from 5.23 mg/L to 12.11 mg/L. In March 2021, the concentrations of chloride at 10 cm ranged from 3.15 mg/L to 29.02 mg/L.

A mean of 7.69 mg/L of NO_3-N was observed at 10 cm. In June 2020, the concentrations of NO_3-N at 10 cm ranged from 7.67 mg/L to 11.41 mg/L (Figure 4). In July 2020, the concentrations of NO_3-N at 10 cm ranged from below detection limit to 7.06 mg/L. In September

2020, the concentrations of NO_3-N at 10 cm ranged from below detection limit to 0.29 mg/L. In November 2020, the concentrations of NO_3-N at 10 cm ranged from below detection limit to 0.48 mg/L. In March 2021, the concentrations of NO_3-N at 10 cm ranged from 0.30 mg/L to 7.00 mg/L.

A mean of 16.69 mg/L of chloride was observed at 20 cm below the streambed. In June 2020, the concentrations of chloride at 20 cm below surface ranged from 23.94 mg/L to 27.21 mg/L. In July 2020, the concentrations of chloride at 20 cm ranged from 15.77 mg/L to 26.16 mg/L. In September 2020, the concentrations of chloride at 20 cm ranged from 3.44 mg/L to 24.55 mg/L. In November 2020, the concentrations of chloride at 20 cm ranged from5.48 mg/L to 11.96 mg/L. In March 2021, the concentrations of chloride at 20 cm ranged from 3.23 mg/L to 22.18 mg/L.

A mean of 5.76 mg/L of NO_3-N was observed at 20 cm. In June 2020, the concentrations of NO_3-N at 20 cm ranged from 9.57 mg/L to 12.38 mg/L. In July 2020, the concentrations of NO_3-N at 20 cm ranged from 15.77 mg/L to 26.16 mg/L. In September 2020, the concentrations of NO_3-N at 20 cm ranged from below detection limit to 0.31 mg/L. In November 2020, the concentrations of NO_3-N at 20 cm ranged from below detection limit to 0.48 mg/L. In March 2021, the concentrations of NO_3-N at 20 cm ranged from 0.36 mg/L to 4.26 mg/L.

A mean of 13.29 mg/L of chloride was observed at 30 cm below the streambed. In June 2020, the concentrations of chloride at 30 cm below surface ranged from 22.06 mg/L to 25.69 mg/L. In July 2020, the concentrations of chloride at 30 cm ranged from 4.05 mg/L to 22.63 mg/L. In September 2020, the concentrations of chloride at 30 cm ranged from 2.95 mg/L to 12.79 mg/L. In November 2020, the concentrations of chloride at 30 cm ranged from 4.22 mg/L

to 12.03 mg/L. In March 2021, the concentrations of chloride at 30 cm ranged from 4.95 mg/L to 20.57 mg/L.

A mean of 2.40 mg/L of NO_3-N was observed at 30 cm. In June 2020, the concentrations of NO_3-N at 30 cm ranged from 2.88 mg/L to 11.67 mg/L. In July 2020, the concentrations of NO_3-N at 30 cm ranged from below detection limit to 7.62 mg/L. In September 2020, the concentrations of NO_3-N at 30 cm were below detection limit throughout the stream at this depth. In November 2020, the concentrations of NO_3-N at 30 cm ranged from below detection limit to 0.49 mg/L. In March 2021, the concentrations of NO_3-N at 30 cm ranged from 0.35 mg/L to 3.67 mg/L.

A mean of 12.60 mg/L of chloride was observed at 50 cm below the streambed during this sampling period. In June 2020, the concentrations of chloride at 50 cm below surface ranged from 13.31 mg/L to 21.93 mg/L. In July 2020, the concentrations of chloride at 50 cm ranged from 12.82 mg/L to 23.18 mg/L. In September 2020, the concentrations of chloride at 50 cm ranged from 7.19 mg/L to 12.91 mg/L. In November 2020, the concentrations of chloride at 50 cm ranged from 4.43 mg/L to 12.01 mg/L. In March 2021, the concentrations of chloride at 50 cm ranged from 2.82 mg/L to 12.36 mg/L.

A mean of 0.39 mg/L of NO_3-N was observed at 50 cm depth below the surface. In June 2020, the concentrations of NO_3-N at 50 cm ranged from 1.37 mg/L to 9.21 mg/L. In July 2020, the concentrations of NO_3-N at 50 cm ranged from 2.53 mg/L to 7.76 mg/L. In September 2020, the concentrations of NO_3-N at 50 cm ranged from below detection limit to 0.30 mg/L. In November 2020, the concentrations of NO_3-N at 50 cm ranged from below detection limit to 0.47 mg/L. In March 2021, the concentrations of NO_3-N at 50 cm ranged from below detection limit to 2.73 mg/L.

Mixing Model

Percent Surface Water Based on Chloride

A mixing model was developed using measured chloride and nitrate as nitrogen concentrations in samples taken from the T3 stream, T3 HZ, and riparian wells (to represent groundwater concentrations) (Equation 1,2). This model first used average measured chloride concentrations at each depth for each sampling month to determine the amount of surface water infiltration along depth in the HZ. The model then used this ratio of infiltration to calculate the amount of NO_3-N expected to be observed at each depth in the HZ based on that level of mixing. The model was only applicable in cases where these average concentrations of chloride and NO_3-N fell within the bounds of the two endmember concentrations of the stream and groundwater during each time period. Because of this, certain depths within the HZ during certain months could not be assessed for infiltration or expected NO_3-N within the model. The average percent of infiltrating surface water could not be calculated for 10 cm and 20 cm depth in the HZ in July and September 2020, 30 cm depth in the HZ in September and November 2020, or 50 cm depth in the HZ in September 2020 because the majority of the concentrations measured at these depths were greater than those observed in the stream. The exception to this were the November 2020 samples at 30 cm depth, which exhibited concentrations of chloride in the HZ that did fall within the observed stream and groundwater endmember concentrations, but due to insufficient sample availability, in this specific case, only two samples were available rather than the minimum three needed for model calculation, so could not be used in the model. Additionally, the 30-cm sampling depth at well 2 during September and November 2020 was not yielding samples; so, there was an insufficient number of samples in either of these months to model the level of surface water infiltration or the associated expected NO_3-N at this depth.

The average percent surface water calculated to have sourced the streambed flow at 10 cm depth in the HZ in June 2020 was 75.6% and at 20 cm depth in the HZ in June 2020 was 78.1%. The average percent of surface water calculated to have sourced the streambed flow at 30 cm depth in the HZ in June 2020 was 72.9% and at 50 cm depth in the HZ in June 2020 was 53.7%.

The average percent of surface water calculated to source 30 cm depth in the HZ in July 2020 was 51.0%. The average percent of surface water calculated to source 50 cm depth in the HZ in July 2020 was 68.0%.

The average percent of surface water calculated to source 10 cm depth in the HZ in November 2020 was 32.1% and at 20 cm depth in the HZ in November 2020 was 31.6%. The average percent of surface water calculated to source 50 cm depth in the HZ in November 2020 was 27.6%.

The average percent of surface water calculated to source 10 cm depth in the HZ in March 2021 was 50.2 % and at 20 cm depth was 43.5%. The average percent of surface water calculated to source 30 cm depth in the HZ in March 2021 was 42.3% and to source 50 cm depth was 36.0% (Figure 5).

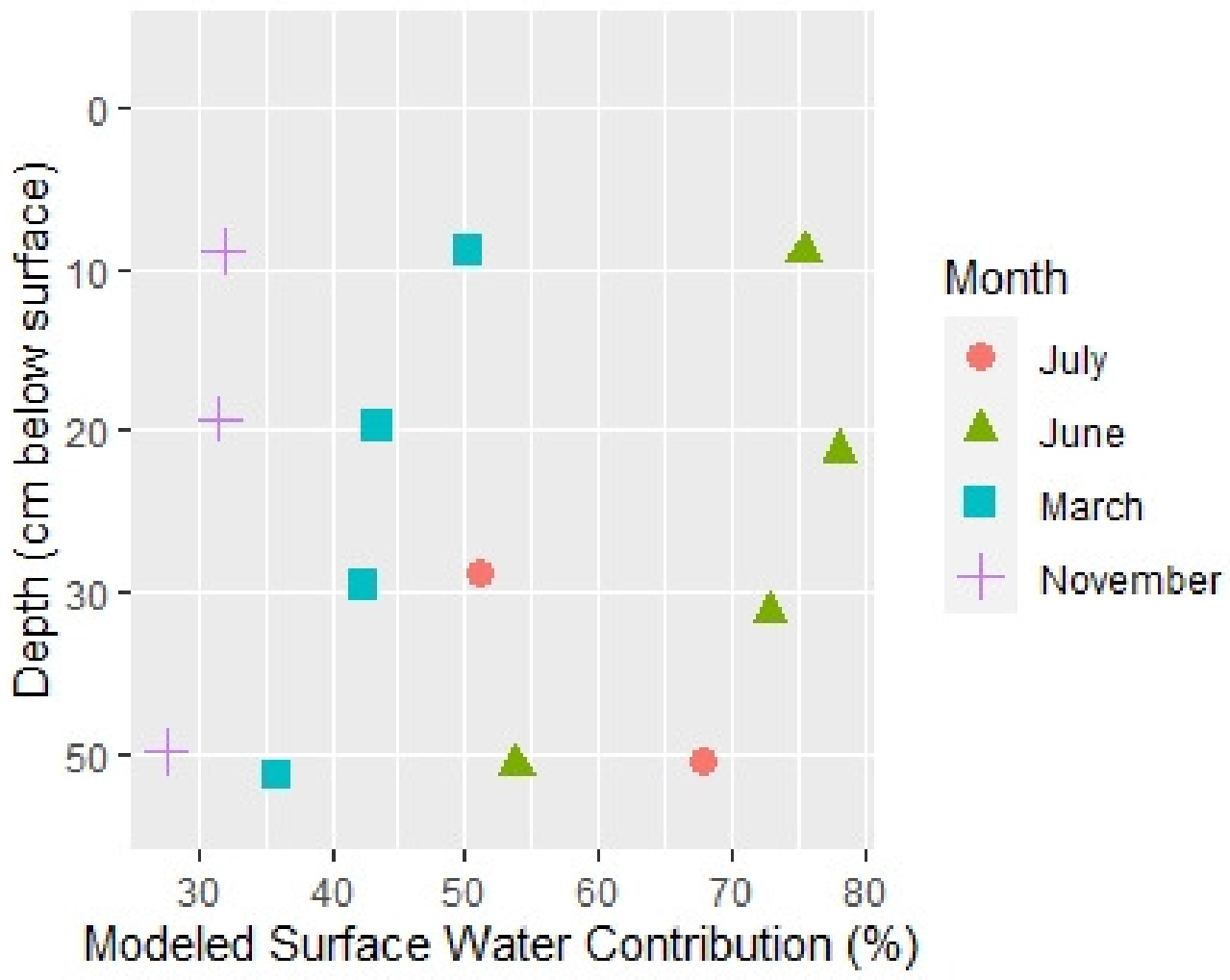

Figure 5 Modeled percentage of surface water infiltration within the T3 HZ (Equation 1). The model could not be calculated for September.

Expected NO_3-N

Based on the calculated chloride levels at each depth of the HZ at T3 noted in the previous section, it is expected that there should have then been a concentration of 12.20 mg/L of NO_3-N observed at 10 cm depth, a concentration of 12.58 mg/L NO_3-N observable at 20 cm, 11.80 mg/L of NO_3-N was expected to be observable at 30 cm depth, and 8.92 mg/L of NO_3-N was expected to be observable at 50 cm depth in June.

The surface water sourcing calculations indicated that 4.94 mg/L of NO_3-N was expected to be observed at 30 cm depth in the HZ and a concentration of 6.23 mg/L of NO_3-N was expected at 50 cm depth in July.

The chloride level calculations indicated that at 20 cm depth in the HZ, 0.63 mg/L NO_3-N was expected and at 50 cm depth, 0.60 mg/L of NO_3-N was expected to be observable in November.

The chloride level calculations indicated that 5.82 mg/L of NO_3-N was expected at 10 cm, 5.62 mg/L NO_3-N was expected at 20 cm depth, 5.58 mg/L of NO_3-N was expected to be observed at 30 cm depth, and a concentration of 5.38 mg/L was expected at 50 cm depth in the HZ in March (Figure 6).

While a general trend of decreasing surface water infiltration was seen along the depth of the HZ for most months, in June, there was an increase in surface water infiltration and mixing, rather than a decrease, at 20 and 30 cm depth. These trends mirrored the measured NO_3-N concentrations observed throughout the depth of the HZ, but the measured concentrations were consistently lower than those calculated in the model (Appendix A).

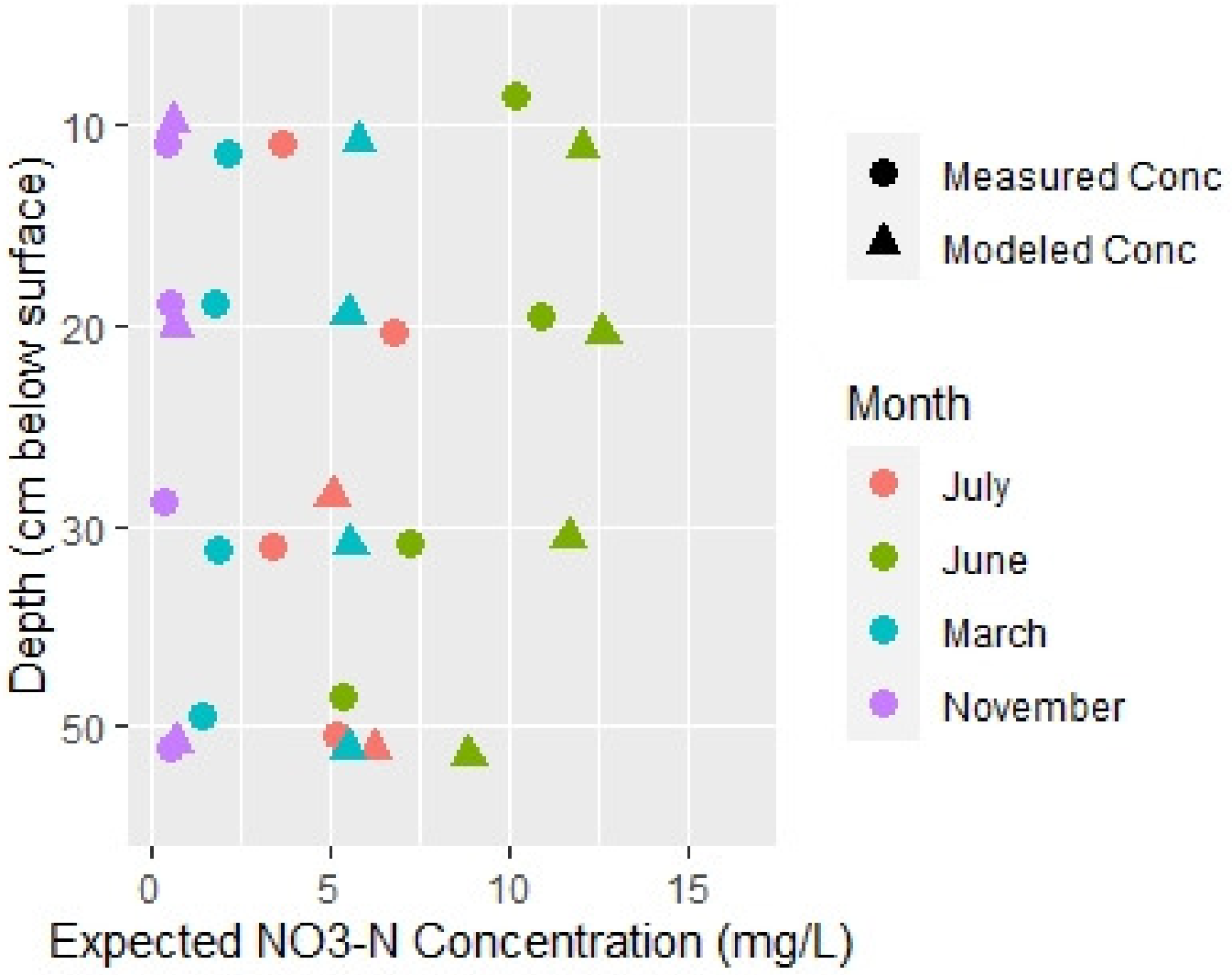

Figure 6 Expected nitrate as nitrogen concentration for mixing in the hyporheic zone at T3 modeled against the average NO_3-N concentrations that were observed at the site throughout the sampling period (Equation 2).

CHAPTER IV: DISCUSSION

The questions that this study aimed to answer were what are the dynamics of water mixing in the HZ and how might that mixing relate to the removal of nitrate from stream systems. In the stream itself, the measured chloride and NO_3-N concentrations did exhibit trends that support mixing between surface and groundwater in the HZ. The model developed for this study supported that there is also NO_3-N removal in the HZ of the stream. The data suggest that mixing waters in the HZ can be correlated to NO_3-N removal in this shallow subsurface flow zone.

Movement of Water in the HZ

Chloride serves as a reliable tracer tracking the movement of surface water down through the depth of the HZ. The measured concentrations of chloride in the T3 HZ were averaged and used to develop a mixing model that calculated the ratio of infiltrating surface water to upwelling groundwater observed to contribute as a source of water to the mixed flow seen along the depth of the HZ in percentages. Throughout the sampling period, from spring to fall, modeled surface water sourcing percentages along the HZ depth using measured chloride concentrations from the T3 HZ exhibit a consistent pattern of decreasing surface water sourcing along the depth of the HZ in this stream (Figure 5). Measured chloride concentration data show that there is a temporary increase in concentration at 20cm depth, but that otherwise, chloride decreases along the entire depth of the HZ in the T3 stream. This increase in concentration does not equate to an increase in infiltrating surface water, as more water could not suddenly infiltrate to that depth more than it had to the overlying depth. However, while this temporary increase in chloride at 20 cm depth cannot be explained by this study, it has been posited by other studies to potentially be due to geomorphological factors, such as residence time within the HZ flow at this location, and by the multidimensional dynamics of flow within a streambed, which include both flow from

upstream paths as well as surficially-contributing and upwelling, groundwater-waters (Tonina and Buffington, 2007; Zarnetske et al., 2011).

The mixing model showed that there was a consistent temporal pattern of significant infiltration near the streambed-HZ interface, with a decrease of sourcing from surface water to the mixing zone along depth. In the summer months, surface water contribution along the entire HZ depth were much greater than in the winter, and in spring, the level of surface water contribution was somewhere in the middle between the summer and winter quantities of contribution. While other studies into this phenomenon vary in their reasons as to why this seasonal pattern is observed, they consistently show that the amount of infiltration sourcing is mainly due to geomorphology, permeability, and groundwater head, but that seasonal water level changes and temperature changes also affect this storage flux and therefore, the direction and magnitude of water flux through the system (Puckett et al., 2008).

However, whether in summer or fall, the model showed that surface water was a source to the HZ and mixing with waters throughout the depth of the HZ. To reiterate, in June 2020, 75.6% of the water at 10 cm depth was contributing surface water and at 50 cm depth, 53.7% of the water in that zone still consisted of surface water contribution. In November, 32.1% of the water at 10 cm depth was contributing surface water while 27.6% of the water sampled at 50 cm depth was surface water contribution. While these lower values of contributing surface water observed in the fall were likely due to the overall lower precipitation levels and stream stage at the time, no matter the time of year, surface water was fully mixing along the depth of the HZ (NIDIS, 2020).

Previous studies have mapped the T3 stream Hyporheic zone to be approximately 50 cm in thickness, since at that depth below the streambed, the geology transitions to till and has a much

lower hydraulic conductivity (Miller et al., 2019). This study assumed that 50 cm is the bottom of the HZ at this site due to this lower hydraulic conductivity in the till and the subsequent difficulty to access and sample this level of the water table, but it is important to note that the interfaces between stream, HZ, and deeper groundwater can be transitory and are not solely reliant on the geology of the subsurface. Not only is the three-dimensional dynamic of geology much more complex than the lateral and longitudinal observations that this study may show along the length of an entire stream or even reach, but the geology of a streambed is constantly shifting based on storm events, erosional patterns, etc. Because of this, the HZ can change in thickness and permeability both spatially and temporally along the length of a stream. Peterson and Hayden, 2018 found that surface water infiltration varied greatly in association with stream stage, groundwater level, and season, irrespective of the actual geology of the HZ in that streambed. For the purposes of this study, and considering the concentrated area of sample collection along the length of the T3 stream, it can be assumed that the HZ maintained a consistent thickness throughout the sampled area. However, over longer reaches of a given stream and a greater time period than the given year of study that this paper explores, the capacity for water mixing and contaminant processing within an HZ could vary. Further study has the potential to more precisely confirm the localized efficacy of each branch of a stream's HZ over time.

Sulfate, while not a conservative ion like chloride, has the potential to indicate an additional source of water to the HZ: deeper groundwater. This is because sulfate exists in higher concentrations in deeper groundwater, where depleted oxygen and longer residence times leads to increased organic decomposition and sulfate release. If the sulfate levels measured in this study area were matched at points of increased concentration with that of an unexpectedly high

chloride concentration, then this would support a potential other deeper groundwater source of chloride to the HZ. While deeper groundwater could be contributing to some extent to this system, the sulfate concentration observed in this study was not able to confirm that because period of higher sulfate concentrations did not consistently correlate to points of higher chloride concentration in the HZ (Table 1). The higher chloride concentrations in the HZ during the study period could be caused by the lower stream stage observed due to the dry conditions in 2020, either via delayed bank storage release at lower stream stage level or, potentially, more concentrated waters and greater precipitations of salt out of the stream waters at this low stream stage level (Chabela and Peterson, 2019). Further study is necessary to support these explanations for increased chloride.

The mixing model used the calculated percent of contributing surface water throughout the HZ to then predict expected average NO_3-N concentrations for each depth of the HZ throughout time based on that amount of calculated surface source contribution and in-zone mixing. The thorough mixing of water along the depth of the HZ means both that the nitrate-rich surface waters in this stream are reaching the bottom of the HZ and that the entirety of the HZ is contributing to the processing and removal of NO_3-N in the streambed.

Change in NO_3-N Concentration in the HZ

In the peak of the growing season, measured NO_3-N concentrations in the HZ at T3 show a distinct trend from surface to depth, with highest concentrations seen at the surface, lowest in groundwater, and a general decreasing trend through the HZ, with the exception of 20 cm depth. This trend mirrors that of the measured chloride concentrations along depth, and the associated modeled surface water contribution levels along depth.

This study is not able to determine why the patterns of decreasing NO_3-N and decreasing chloride are aligned along depth, but this spike in NO_3-N at 20 cm depth during the months of June, July, September, and November specifically is potentially caused by a brief addition of another water source inputting to the HZ at this point or a temporary change in the mixing dynamics at this location (Peterson and Hayden, 2018). However, further analysis is required to definitively support that change in the pattern because localized variations in flow patterns and residence times of the flow within the HZ, which were not considered during this study, could also be contributing to this isolated point of increase in the HZ (Tonina and Buffington, 2007; Zarnetske et al., 2011). At all depths where the model was not able to be applied because the chloride concentrations were greater than, or in November, insufficient to determine fit within the bounding endmember concentrations, which occurred in at least one month at every depth within the HZ and throughout the entirety of September, these same potential mechanisms for temporary change in chloride can be applied. Since the measured levels of chloride at 20 cm depth still fall within the bounds established by the measured stream and groundwater levels at the site, the model calculations, where the model could be applied, support that a temporary increase of NO_3-N, rather than a significantly different processing mechanism, is manifesting at this depth in the HZ (Krause et al., 2013). Observed NO_3-N concentrations in the HZ are second highest at 10 cm depth, demonstrating the initial infiltration of surface water into the HZ. However, since these 10 cm-depth concentrations are still lower than that of the surficial stream water, and they additionally are lower than the model-predicated NO_3-N levels at this depth, it can be inferred that NO_3-N removal processes begin immediately upon infiltration into the HZ. At 30 cm depth, mean NO_3-N concentrations decrease again to below that of 10 cm depth, and

continue to decrease at 50 cm depth, at the bottom of the HZ. This same trend is observable at lower concentrations in the spring and fall.

The model-estimated levels of NO_3-N were what was expected to be seen at each point in the HZ based on the level of mixing that occurred at each depth. While the model did exhibit the same trend in NO_3-N concentration along depth as that of the measured samples from the stream, it also consistently estimated higher levels of NO_3-N than what was actually observed in the T3 HZ (Figure 6). In fact, it consistently exhibited greater than 10% higher concentrations of NO_3-N than what was measured in the HZ, supporting that NO_3-N removal is occurring along depth and that whatever process is causing the removal of NO_3-N in the HZ is not dilution, which would require both a consistent decrease in NO_3-N concentration along depth as well as the measured NO_3-N concentrations to be within 10% of the modeled values for NO_3-N (Appendix A) (Peterson and Hayden, 2018). In the fall and winter, when vegetation is at a minimum in the area surrounding the stream, this trend of decreasing NO_3-N concentration along depth, with a slight increase at 20 cm depth, is observed on a more subtle, and smaller, scale. This consistency in trend despite the season is likely due to the fact that there are multiple contributing mechanisms to nitrate removal. While plant uptake is one of these mechanisms, microbial assimilation and microbial denitrification are others that could be occurring year-round to cause nitrate removal to occur in the HZ whether vegetation is present or not (Winter et al., 1998; Miller et al., 2019).

The T3 streambed, unlike the riparian zone, was mostly void of benthic vegetation. While burial of transported organic matter could contribute to a microbial impact on NO_3-N processing along the depth of the HZ, plant assimilation within the HZ in the streambed itself is unlikely. The decreasing concentrations of NO_3-N along depth, in addition to this lack of vegetation in the stream, supports that NO_3-N removal processes, such as denitrification, were more likely to

cause the NO_3-N removal in this system than plant assimilation (Klocker et al., 2009; Gift et al., 2010). More study is required to confirm this specific process for removal, however.

Differences in longitudinal mixing and NO_3-N concentrations could not be definitively observed between the wells themselves. There was very little difference among the three in-stream wells based on measured NO_3-N concentrations at 20 and 30 cm depth at T3. At 10 cm depth, there was a discernable decrease in NO_3-N as flow moved downstream, supporting the efficiency of NO_3-N removal processes in the HZ at the streambed interface as water flows downstream. At 50 cm depth, the center well showed markedly lower NO_3-N concentrations than the wells both upstream and downstream of its location, but the upstream and downstream wells were similar to each other in NO_3-N concentration, so this anomaly could not be further explained based on this dataset. It is notable that while the upstream and downstream wells exhibited very similar concentrations along depth throughout the seasons, with somewhat distinct groupings of concentrations at each depth, the middle well was much more variable along depth among the months. Other studies have found longitudinal chemical processing to occur in the HZ, but further study using a more reliable tracer, such as the conservative ion bromide, is required to solidify these longitudinal variations (Winter et al., 1998; U.S. Environmental Protection Agency (EPA), 2003; Peterson and Hayden, 2018). Additionally, the longitudinal variations in chemical characteristics are not solely based on longitudinal flow, but also the depth-wise, and to a much lesser extent, lateral flow attributes. This could contribute to a compounding or nullifying of variations between wells along the length of the stream.

NO_3-N levels in the riparian subsurface were comparatively very low and indicate that HZ mixing does not extend substantially into the banks of the stream in this matrix environment (Appendix A). These low levels of NO_3-N in the riparian zone demonstrate that groundwater

dominates the riparian landscape almost directly up to the bank margin. Hydraulic head data show groundwater movement to the stream. The mixing model supports the upwelling of groundwater, which would indicate a minimal lateral exchange of stream water into the banks (Peterson et al., 2018). While some small amount of mixing inevitably occurs between surface water and groundwater at the cusp of the streambank, that mixing is not more impactful on the overall processing of NO_3-N in these environments than the nitrifying, denitrifying, and plant-uptake related processes that can be observed independently in the groundwater and HZ.

A limitation of the model used in this study is that it used average measured chloride and NO_3-N concentrations to calculate average expected surface water contribution percentages and NO_3-N concentrations at depth. Averages were used to make these calculations because of the limited sample size, since most sampling locations only had one to two samples for each depth in each month. The averages are sufficient to answer the questions at hand but do mean that accuracy versus precision was emphasized by the results of this study.

Stream stage has been shown to contribute to denitrification in the HZ. Higher stream stage can contribute to more thick and frequent organic detritus deposits, creating an optimal environment for denitrification to occur in the streambed (Baker and Vervier, 2004). However, as previously noted the stream stage was low and stagnant throughout the sampling period. Using a nearby stream as a proxy, because stream stage is not regularly measured at the T3 site, Six Mile Creek precipitation and stream gage data show that on the sampling dates, rainfall was consistently very low and stream stage was also consistently low (Table 2). This could mean that whatever concentrations of NO_3-N were observed in the HZ during this study could be lower than those observed in a wetter year, and further study is required to determine the efficiency of nitrate removal in streams with differing stages.

Table 2: Rainfall and Stream Stage at Proxy-Stream Six Mile Creek on the T3-HZ Sample Dates (Personal Communication, 2021)

Sample Date at T3	Rainfall at Six Mile Creek by this date (cm)	Stream Stage at Six Mile Creek on this Date (ft)
6/17/2020	51.6	1.72
6/24/2020	n.a.	n.a.
7/8/2020	53.3	0.75
7/17/2020	68.1	0.04
7/22/2020	70.3	0.57
9/3/2020	n.a.	n.a.
11/10/2020	91.7	0.73
3/6/2021	8.2	0.92

CHAPTER V: CONCLUSIONS

Conclusions

The observed concentrations and the resulting modeled concentrations support that there is mixing of surface water and upwelling groundwater within the thickness the HZ of T3. This mixing can also be correlated to a general removal of NO_3-N in the HZ, though further research is needed to parse out the intricate mechanism of nitrogen cycling processes contributing to the removal observed in this shallow subsurface zone. The evidence supports that surface water contributes the greatest amount of water to the HZ near the boundary of the streambed and the HZ and groundwater contributes comparatively little to this surface-adjacent zone. Along depth, the contribution of surface water decreases and the quantity of deeper, upwelling groundwater in the mix increases. There is a positive relationship between depth of the HZ and a removal of NO_3-N in this zone. This same relationship can be observed downstream. Additional investigation is warranted to assess whether the removal is seen longitudinally due to mixing in the flow or if another factor is at play in that mixing dynamic.

Riparian HZ interaction in this stream is limited. The data indicate that groundwater movement within the banks of a stream is mainly driven by groundwater processes, and this water interacts less with the stream itself than the HZ directly below the streambed does. The mixing from this minimal level of interaction likely contributes little to NO_3-N removal in riparian HZs.

Future Work

It is recommended that future studies apply a bromide tracer continuous injection test at baseflow conditions for a 10-hour period to assist in determining how deeply the stream water infiltrates into the HZ versus the groundwater upwelling to the stream from beneath the HZ.

Since bromide does not naturally occur at high concentrations, it is an effective tracer to use in determining direction and length of flow of water through the HZ. The bromide tracer could be used to determine how deeply the stream water infiltrates. Bromide concentrations in a water well at comparable depth in the riparian zone adjacent to the stream test site could be analyzed to determine the distance of travel and the extent of stream water/hyporheic exchange with nearby soils (Davis et al., 1985; Ackerman et al., 2015; Peter et al., 2019).

REFERENCES

Ackerman, J.R., Peterson, E.W., Van der Hoven, S., and Perry, W.L., 2015, Quantifying nutrient removal from groundwater seepage out of constructed wetlands receiving treated wastewater effluent: Environmental Earth Sciences, v. 74, p. 1633–1645, doi:10.1007/s12665-015-4167-3.

Anderson, M.P., 2005, Heat as a ground water tracer: Ground Water, v. 43, p. 951–968, doi:10.1111/j.1745-6584.2005.00052.x.

Baker, M.A., and Vervier, P., 2004, Hydrological variability, organic matter supply and denitrification in the Garonne River ecosystem: Freshwater Biology, v. 49, p. 181–190, doi:10.1046/j.1365-2426.2003.01175.x.

Chabela, L.P., and Peterson, E.W., 2019, and Bank Storage along a Meandering Stream:

Clausen, J.C., Guillard, K., Sigmund, C.M., and Dors, K.M., 2000, Water Quality Changes from Riparian Buffer Restoration in Connecticut: Journal of Environmental Quality, v. 29, p. 1751–1761, doi:10.2134/jeq2000.00472425002900060004x.

David, M.B., and Gentry, L.E., 2000, Anthropogenic Inputs of Nitrogen and Phosphorus and Riverine Export for Illinois, USA: Journal of Environmental Quality, v. 29, p. 494–508, doi:10.2134/jeq2000.00472425002900020018x.

Davis, S.N., Campbell, D.J., Bentley, H.W., and Flynn, T.J., 1985, An introduction to groundwater tracers. EPA: , p. 219.

Day, J.W., Yañéz Arancibia, A., Mitsch, W.J., Lara-Dominguez, A.L., Day, J.N., Ko, J.Y., Lane, R., Lindsey, J., and Lomeli, D.Z., 2003, Using Ecotechnology to address water quality and wetland habitat loss problems in the Mississippi basin: A hierarchical approach: Biotechnology Advances, v. 22, p. 135–159, doi:10.1016/j.biotechadv.2003.08.012.

Gift, D.M., Groffman, P.M., Kaushal, S.S., and Mayer, P.M., 2010, Denitrification potential, root Biomass, and organic matter in degraded and restored urban riparian zones: Restoration Ecology, v. 18, p. 113–120, doi:10.1111/j.1526-100X.2008.00438.x.

Hill, A.R., Labadia, C.F., and Sanmugadas, K., 1998, Hyporheic zone hydrology and nitrogen dynamics in relation to the streambed topography of a N-rich stream: Biogeochemistry, v. 42, p. 285–310, doi:10.1023/A:1005932528748.

Kaushal, S.S., Groffman, P.M., Mayer, P.M., Striz, E., and Gold, A.J., 2008, Effects of stream restoration on denitrification in an urbanizing watershed: Ecological Applications, v. 18, p. 789–804, doi:10.1890/07-1159.1.

Klocker, C.A., Kaushal, S.S., Groffman, P.M., Mayer, P.M., and Morgan, R.P., 2009, Nitrogen uptake and denitrification in restored and unrestored streams in urban Maryland, USA: Aquatic Sciences, v. 71, p. 411–424, doi:10.1007/s00027-009-0118-y.

Krause, S., Tecklenburg, C., Munz, M., and Naden, E., 2013, Streambed nitrogen cycling beyond the hyporheic zone: Flow controls on horizontal patterns and depth distribution of nitrate and dissolved oxygen in the upwelling groundwater of a lowland river: Journal of Geophysical Research: Biogeosciences, v. 118, p. 54–67, doi:10.1029/2012JG002122.

Lapham, W.W., 1989, Use of temperature profiles beneath streams to determine rates of vertical

ground-water flow and vertical hydraulic conductivity: US Geological Survey Water-Supply Paper, v. 2337, doi:10.3133/wsp2337.

Lautz, L.K., and Fanelli, R.M., 2008, Seasonal biogeochemical hotspots in the streambed around restoration structures: Biogeochemistry, v. 91, p. 85–104, doi:10.1007/s10533-008-9235-2.

Maas, B., Peterson, E.W., Honings, J., Oberhelman, A., Oware, P., Rusthoven, I., and Watson, A., 2019, Differentiation of surface water and groundwater in a karst system using anthropogenic signatures: Geosciences (Switzerland), v. 9, p. 1–16, doi:10.3390/geosciences9040148.

Mason, S.J.K., McGlynn, B.L., and Poole, G.C., 2012, Hydrologic response to channel reconfiguration on Silver Bow Creek, Montana: Journal of Hydrology, v. 438–439, p. 125–136, doi:10.1016/j.jhydrol.2012.03.010.

Miller, J., Peterson, E.W., and Budikova, D., 2019, Diurnal and seasonal variation in nitrate-nitrogen concentrations of groundwater in a saturated buffer zone: Hydrogeology Journal, v. 27, p. 1373–1387, doi:10.1007/s10040-018-1907-y.

O'Reilly, CM. 2021. Six Mile Creek Stream Gauge and Precipitation Data (Personal Communcation).

Pescimoro, E., Boano, F., Sawyer, A.H., and Soltanian, M.R., 2019, Modeling Influence of Sediment Heterogeneity on Nutrient Cycling in Streambeds: Water Resources Research, v. 55, p. 4082–4095, doi:10.1029/2018WR024221.

Peter, K.T., Herzog, S., Tian, Z., Wu, C., McCray, J.E., Lynch, K., and Kolodziej, E.P., 2019, Evaluating emerging organic contaminant removal in an engineered hyporheic zone using high resolution mass spectrometry: Water Research, v. 150, p. 140–152, doi:10.1016/j.watres.2018.11.050.

Peterson, B.J. et al., 2001, Control of nitrogen export from watersheds by headwater streams: Science, v. 292, p. 86–90, doi:10.1126/science.1056874.

Peterson, E.W., and Benning, C., 2013, Factors influencing nitrate within a low-gradient agricultural stream: Environmental Earth Sciences, v. 68, p. 1233–1245, doi:10.1007/s12665-012-1821-x.

Peterson, E.W., and Hayden, K.M., 2018, Transport and fate of nitrate in the streambed of a low-gradient stream: Hydrology, v. 5, p. 34–38, doi:10.3390/hydrology5040055.

Peterson, E.W., Ludwikowski, J., and Chabela, L.P., 2018, Transport and Fate of Chloride from Road Salt within a Mixed Urban and Agricultural Watershed : Assessing the Influence of Chloride Background – Problems with Chloride (Cl -): , p. 1123–1135, doi:10.1007/s10040-018-1732-3.

Puckett, L.J., Zamora, C., Essaid, H., Wilson, J.T., Johnson, H.M., Brayton, M.J., and Vogel, J.R., 2008, Transport and fate of nitrate at the ground-water/surface-water interface: Journal of Environmental Quality, v. 37, p. 1034–1050, doi:10.2134/jeq2006.0550.

Ren, J., Zhang, W., Yang, J., and Zhou, Y., 2019, Using water temperature series and hydraulic heads to quantify hyporheic exchange in the riparian zone: Hydrogeology Journal, v. 27, p. 1419–1437, doi:10.1007/s10040-019-01934-z.

Sabater, S. et al., 2003, Nitrogen removal by riparian buffers along a European climatic gradient: Patterns and factors of variation: Ecosystems, v. 6, p. 20–30, doi:10.1007/s10021-002-0183-8.

Seeger, E.M., Maier, U., Grathwohl, P., Kuschk, P., and Kaestner, M., 2013, Performance evaluation of different horizontal subsurface flow wetland types by characterization of flow behavior, mass removal and depth-dependent contaminant load: Water Research, v. 47, p.

769–780, doi:10.1016/j.watres.2012.10.051.

Smith, M.S., and Tiedje, J.M., 1979, Phases of denitrification following oxygen depletion in soil: Soil Biology and Biochemistry, v. 11, p. 261–267, doi:10.1016/0038-0717 (79)90071-3.

Tonina, D., and Buffington, J.M., 2007, Hyporheic exchange in gravel bed rivers with pool-riffle morphology: Laboratory experiments and three-dimensional modeling: Water Resources Research, v. 43, doi:10.1029/2005WR004328.

Triska, F.J., Kennedy, V.C., Avanzino, R.J., and Zellweger, G.W., 1989, Retention and Transport of Nutrients in a Third-Order Stream in Northwestern California : Hyporheic Processes and Kenneth E . Bencala Published by : Wiley on behalf of the Ecological Society of America Stable URL : https://www.jstor.org/stable/1938120 REF: v. 70, p. 1893–1905.

Turner, R.E., and Rabalais, N.N., 1991, Changes in Mississippi River Water Quality This Century: BioScience, v. 41, p. 140–147, doi:10.2307/1311453.

U.S. Environmental Protection Agency (EPA), 2003, Tracer-Test Planning Using the Efficient Hydrologic Tracer-Test Design (EHTD) Program: Environmental Protection, http://www.epa.gov/ncea/.

Vitousek, P.M. et al., 2002, Towards an ecological understanding of biological nitrogen fixation: Biogeochemistry, v. 57–58, p. 1–45, doi:10.1023/A:1015798428743.

Ward, B.B., 2013, Nitrification: Encyclopedia of Ecology, p. 351–358, doi:10.1016/B978-0-12-409548-9.00697-7.

Winter, T.C., Harvey, J.W., Franke, O.L., and Alley, W.M., 1998, Ground Water Surface Water and A Single Resource: USGS Publications, p. 79, http://pubs.usgs.gov/circ/circ1139/pdf/circ1139.pdf.

Zak, D. et al., 2018, Nitrogen and Phosphorus Removal from Agricultural Runoff in Integrated

Buffer Zones: Environmental Science and Technology, v. 52, p. 6508–6517, doi:10.1021/acs.est.8b01036.

Zaramella, M., Packman, A.I., and Marion, A., 2003, Application of the transient storage model to analyze advective hyporheic exchange with deep and shallow sediment beds: Water Resources Research, v. 39, p. 1–12, doi:10.1029/2002WR001344.

Zarnetske, J.P., Haggerty, R., Wondzell, S.M., and Baker, M.A., 2011, Dynamics of nitrate production and removal as a function of residence time in the hyporheic zone: Journal of Geophysical Research: Biogeosciences, v. 116, p. 1–13, doi:10.1029/2010JG001356.

APPENDIX A: SAMPLE DATA AND MODEL CALCULATIONS

Table 3: Measured Sample Concentrations of Chloride and Nitrate as Nitrogen

Sample ID	Chloride (mg/L)	NO_3-N (mg/L)	Sample Location (Stream or Well)	Month	Depth (cm below surface [cmbs])
3_6_21_W1_10	3.1512	0.295	1	March	10
3_6_21_W1_20	3.2363	0.356	1	March	20
3_6_21_W1_30	4.9476	0.353	1	March	30
3_6_21_W1_50	2.8223	0.24	1	March	50
3_6_21_W2_10	12.7918	0.296	2	March	10
3_4_21_W2_10	15.3664	1.108	2	March	10
3_6_21_W2_20	13.9004	0.518	2	March	20
3_6_21_W2_50	12.3615	n.a.	2	March	50
3_6_21_W3_10	29.017	7.002	3	March	10
3_6_21_W3_20	22.1803	4.263	3	March	20
3_6_21_W3_30	20.5677	3.67	3	March	30
3_6_21_W3_50	17.4773	2.725	3	March	50
3_6_21_12C	5.8584	4.272	12c	March	228.6
3_6_21_STREAM	29.861	7.36	stream	March	0
6_24_W1_10	26.6933	11.408	1	June	10
6_24_W1_20	27.2096	12.377	1	June	20
6_24_W1_30	25.6879	11.672	1	June	30
6_24_W1_50	21.9319	9.209	1	June	50
6_24_W2_10	23.7732	10.684	2	June	10
6_24_W2_20	23.9411	9.572	2	June	20
6_24_W2_50	13.3131	1.371	2	June	50
6_24_W3_10	20.3305	7.673	3	June	10
6_24_W3_10	28.1976	11.01	3	June	10
6_24_W3_30	22.0615	2.879	3	June	30
6_17_12A	5.6166	n.a.	12a	June	381
6_17_12B	4.1477	0.568	12b	June	304.8
6_17_12C	4.0452	0.894	12c	June	228.6
6_24_STREAM	31.1189	15.059	stream	June	0
6_17_STREAM	34.2625	16.636	stream	June	0
7_17_W1_10	4.4799	0.473	1	July	10
7_8_W1_10	11.2351	n.a.	1	July	10
7_8_W1_20	15.7743	2.418	1	July	20
7_17_W1_30	4.0533	0.451	1	July	30

7_8_W1_30	11.2993	2.205	1	July	30
7_8_W1_50	12.8261	2.532	1	July	50
7_8_W2_10	25.6611	10.055	2	July	10
7_17_W2_20	25.1341	9.525	2	July	20
7_8_W2_20	26.1589	n.a.	2	July	20
7_8_W3_10	28.6207	0.615	3	July	10
7_8_W3_20	22.621	7.845	3	July	20
7_8_W3_20_DUPLICATE	22.7359	7.858	3	July	20
7_17_W3_30	22.6307	7.618	3	July	30
7_8_W3_30	16.2731	n.a.	3	July	30
7_17_W3_50	23.1765	7.76	3	July	50
7_8_12A	5.6977	0.886	12a	July	381
7_8_12B	3.1543	0.548	12b	July	304.8
7_22_12B	4.2217	0.897	12b	July	304.8
7_8_12C	3.2272	0.604	12c	July	228.6
7_22_12C	4.3945	1.506	12c	July	228.6
7_17_12D	3.1374	0.656	12d	July	152.4
7_22_12D	4.3477	1.639	12d	July	152.4
7_22_STREAM	23.2934	7.857	stream	July	0
T3_7_22_STREAM	23.5405	7.858	stream	July	0
7_8_STREAM	31.6111	8.266	stream	July	0
7_17_STREAM	27.1742	10.699	stream	July	0
9_3_W1_10	3.5708	n.a.	1	September	10
9_3_W1_20	3.4358	n.a.	1	September	20
9_3_W1_30	2.9525	n.a.	1	September	30
9_3_W1_50	7.1939	0.299	1	September	50
9_3_W2_10	7.767	0.288	2	September	10
9_3_W2_20	7.0633	n.a.	2	September	20
9_3_W2_50	12.6006	0.282	2	September	50
9_3_W3_10	11.4651	0.279	3	September	10
9_3_W3_20	24.5451	0.307	3	September	20
9_3_W3_30	12.7861	n.a.	3	September	30
9_3_W3_50	12.9135	n.a.	3	September	50
9_3_12B	4.8093	0.408	12b	September	304.8
9_3_12C	3.978	0.414	12c	September	228.6
9_3_STREAM	6.1976	n.a.	stream	September	0
11_10_w1_10	5.2331	0.478	1	November	10
11_10_w1_20	5.4823	n.a.	1	November	20
11_10_w1_30	4.2252	n.a.	1	November	30
11_10_w1_50	4.4294	n.a.	1	November	50
11_10_w2_10	12.1084	n.a.	2	November	10

11_10_w2_20	11.6055	0.481	2	November	20
11_10_w2_50	12.0136	n.a.	2	November	50
11_8_w3_10	11.9257	n.a.	3	November	10
11_8_w3_20	11.9644	n.a.	3	November	20
11_8_w3_30	12.0343	0.489	3	November	30
11_8_w3_50	10.6767	0.474	3	November	50
11_8_12A			12a	November	381
11_8_12B	3.879	0.318	12b	November	304.8
11_8_12C	4.5957	0.343	12c	November	228.6
11_8_12D			12d	November	152.4
11_8_STREAM	20.6921	1.257	stream	November	0

Table 4: Average Calculated Nitrate as Nitrogen Concentrations per Sample Month

Month	Averaged NO_3-N (mg/L)	Depth (cmbs)
March 2021	7.36	0
March 2021	2.17525	10
March 2021	1.712333333	20
March 2021	2.0115	30
March 2021	1.4825	50
March 2021	4.272	228.6
June 2020	15.8475	0
June 2020	10.19375	10
June 2020	10.9745	20
June 2020	7.2755	30
June 2020	5.29	50
June 2020	0.894	228.6
July 2020	8.67	0
July 2020	3.714333333	10
July 2020	6.9115	20
July 2020	3.424666667	30
July 2020	5.146	50
July 2020	1.055	228.6
September 2020	n.a.	0
September 2020	0.2835	10
September 2020	0.307	20
September 2020	n.a.	30
September 2020	0.2905	50
September 2020	0.414	228.6
November 2020	1.257	0
November 2020	0.478	10

November 2020	0.481	20
November 2020	0.489	30
November 2020	0.474	50
November 2020	0.343	228.6

Table 5: Model-Calculated Surface Water Infiltration and Expected NO_3-N Concentration

Modeled % Chloride (Surface Water Infiltration) (Equation 1)	Month	Modeled NO_3-N (Equation 2)	Depth (cmbs)
0.501786629	March 2021	5.821517111	10
0.435177944	March 2021	5.61582949	20
0.423446307	March 2021	5.579602195	30
0.360387845	March 2021	5.384877664	50
0.755892116	June 2020	12.19723276	10
0.781301675	June 2020	12.5771946	20
0.729030275	June 2020	11.79555422	30
0.536861841	June 2020	8.921963541	50
n.a.	July 2020	n.a.	10
n.a.	July 2020	n.a.	20
0.510398694	July 2020	4.941686058	30
0.67958409	July 2020	6.230032848	50
n.a.	September 2020	n.a.	10
n.a.	September 2020	n.a.	20
n.a.	September 2020	n.a.	30
n.a.	September 2020	n.a.	50
0.320570645	November 2020	0.63600157	10
0.316118304	November 2020	0.63193213	20
n.a.	November 2020	n.a.	30
0.276099004	November 2020	0.595354489	50